JOURNAL OF MATERIALS SCIENCE 20 (1985) 3462–3478

Plastic banding in glassy polycarbonate under plane simple shear

C. G'SELL, A. J. GOPEZ
Laboratoire de Physique du Solide, L.A. CNRS No. 155, Ecole des Mines, Parc de Saurupt, 54042 Nancy Cedex, France

Samples of amorphous polycarbonate were tested in plane simple shear at various temperatures (−100 to +150° C) and shear rates (3×10^{-5} to $3 \times 10^{-2} sec^{-1}$). In the glassy state, it was observed that the deformation concentrated at yield inside a single shear band whose elongation and widening phases correspond to well marked stages of the recorded stress–strain curve. Birefringence and X-ray diffraction in the growing band show that the molecular orientation follows a pseudo-affine evolution with the local plastic strain. Although the shear is inhomogeneous during the growth of the shear band, it is fairly uniform inside the band itself, down to the scale of 100 nm. After the band has completed its widening (for an overall shear of about 0.9) the overall shear in the whole specimen is homogeneous and then one can deduce the constitutive equation for steady state plasticity of the glassy material, up to shear strains as large as 2.0. It is characterized by a linear strain hardening whose value, such as the extrapolated yield stress, decreases gradually with temperature.

1. Introduction

Most of the available data concerning the plastic behaviour of glassy polycarbonate were obtained from mechanical testing in uniaxial tension or compression (e.g. Bauwens-Crowet *et al.* [1–3], Titomanlio and Rizzo [4]). These tests not only led to rheological load–elongation curves; they also proved unambiguously that the plastic behaviour of polycarbonate proceeds essentially by the nucleation and growth of shear bands inclined on the tensile (or compression) axis. This basic shear mechanism does appear to be a general feature of the plasticity of glassy polymers as assessed by the extensive set of observations reported in atactic polystyrene in compression [5–12].

However, although tensile or compression tests provide direct evidence of the shear mechanism, they unfortunately give rise to a complex distribution of bands along several (at least two) shear planes. The nucleation of the bands is very ill-controlled, unless using the artefact of making notches or drilling holes in the specimens prior to the test in order to localize banding. Furthermore, the intersection of bands usually disturbs their development. Ultimately, crazing or localized plastic instability cause the failure of the polycarbonate samples at a relatively small strain (about $\varepsilon_{max} = 0.8$ at room temperature). Subsequently, tensile and compression testing can hardly give a complete and quantitative characterization of the shear mode of deformation.

Torsion was also used for the mechanical testing of polycarbonate [13]. This deformation mode favours a unique shear plane normal to the torsion axis and thus avoids the problem of bands intersection. Also in torsion tests, large strains can be attained but the torque–twist curves cannot be simply resolved in terms of shear stress–shear strain curves because of the inherent inhomogeneity of the stresses and strains in this type of test [14].

Recently, a plane simple shear test was

0022–2461/85 $03.00 + .12

developed in this laboratory [15], which gives direct access to the behaviour of a material undergoing simple plastic shear. The test has the following capabilities: (i) application of simple plane shear on a specimen; (ii) ability to obtain immediately shear stress–shear strain curves; (iii) adaptability of the shear testing apparatus to a standared tensile testing machine. This method was proved to be applicable to a large variety of amorphous and semi-crystalline polymers [16].

While the use of the simple shear test has thus far been in the determination of rheological data, the objective of the present study is to take a closer look at the deformation process. By means of *in situ* microscopic observations, we will analyse the kinetics of the development of a unique shear band. Complementary microstructural investigations will help to analyse the orientation of the polymer chains within the band in correlation with the local plastic strain. In the light of these micromechanical and microstructural pieces of information, we will derive the constitutive equation for steady-state plasticity under simple shear.

2. Materials and methods

2.1. Characterization of the polycarbonate polymer

The present work was performed with a commercial grade of Bisphenol A polycarbonate ("polycarbonate" for short) manufactured by Bayer under the trade name "Makrolon" whose main physical characteristics are summarized in Table I. The average molecular weights, $\bar{M}_n$ and $\bar{M}_w$ were obtained from a gel permeation chromatographic test done for this study (with two Shodex 80 M columns, tetrahydrofurane solvent, detection by refractometry, sampling with polystyrene fractions). The tensile testing data were obtained, in this laboratory by the means of a special procedure at constant true strain rate [17]. The high transmission coefficient for visible light can be correlated with the very small degree of crystallinity of the material.This is confirmed by the Wide Angle X-ray Scattering records obtained with a reflexion symmetrical camera (monochromated cobalt radiation), which shows indeed broad amorphous peaks at diffusion vectors $|\mathbf{s}_1| = 1.94\,\text{nm}^{-1}$ and $|\mathbf{s}_2| = 4.72\,\text{nm}^{-1}$ but no crystalline peak at all [18].

The material was received in the form of extruded plates 10 mm thick. This form was preferred to injected pieces, for it leaves the macromolecules free of processing orientation (the residual birefringence of the as-received plates was less than $\Delta n = 5 \times 10^{-5}$).

2.2. Specimens

The first type of specimen was identical to those tested in a previous work [15], as depicted in Fig. 1a. The dimensions of the calibrated part (length $L = 60$ mm, with $h = 4$ mm, thickness $e = 3$ mm) were calculated [15] to eliminate plastic buckling of the specimen, to minimize the effect of the inhomogeneous normal stresses caused by the rotation moment, and to take into account the loading capacity of the tensile testing machine. These samples will be referred to as "standard" specimens in this paper.

The second type of specimen, which we will call the "modified" specimen, was also used in this study in view of the *in situ* optical microscopic observation of the surface at different steps during the deformation process. As shown

TABLE I Physical characteristics of the polycarbonate grade tested in the present study

Properties	Data	Method
Density ($g\,cm^{-3}$)	1.20	DIN 53479
Average molecular weight		GPC
Number based $\bar{M}_n$ ($g\,mol^{-1}$)	15600	
Weight base $\bar{M}_w$ ($g\,mol^{-1}$)	28800	
Polydispersity $\bar{M}_w/\bar{M}_n$	1.86	
Refraction index n	1.586	DIN 53 491
Transmission coeffient for visible light	0.85	DIN 5036
Young's modulus, E (MPa)	2200	DIN 53 454
Tensile yield stress (MPa)	72	at constant
Maximum true stress (MPa)	120	true strain
Maximum true strain	0.65	rate $\dot{\varepsilon} = 1.7 \times 10^{-3}\,sec^{-1}$ [17]

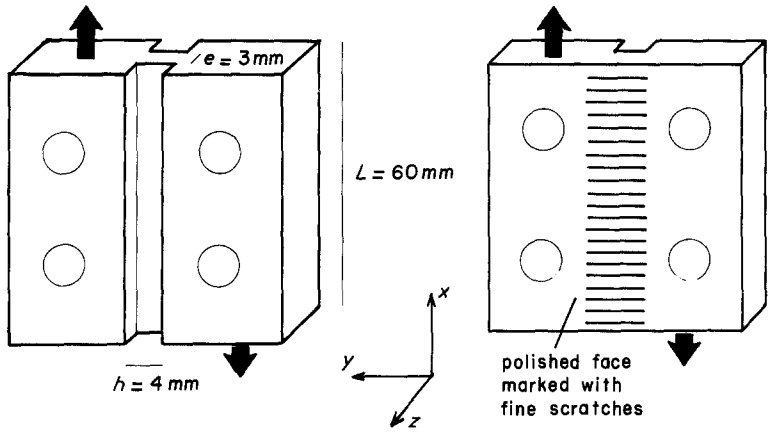

Figure 1 Shape and dimensions of the shear specimens. (a) "Standard" specimens for rheological experiments; (b) "modified" specimens for the microscopic characterization of the deformation.

in Fig. 1b, the shape of this modified sample is such that one face of the calibrated part is level with the gripped heads. This makes possible the fine polishing and the microscopic observation of the exposed face.

2.3. Plane simple shear test

The plane simple shear test [15] provides a direct recording of the variation of the applied shear stress with the overall shear at constant overall shear rate. The applied shear stress (τ) is defined as the force applied, F, per unit area of the calibrated part ($\tau = F/Le$) and the overall shear (γ) is given by the relative displacement of the heads divided by the width of the calibrated part ($\gamma = x/h$). The overall shear rate ($\dot{\gamma}$) is defined as $\dot{\gamma} = \mathrm{d}\gamma/\mathrm{d}t$. In the present work on polycarbonate, the authors improved the original apparatus by designing a special shear transducer (Fig. 2) which made possible the measurement of the shearing displacement, x, on the specimen rather than on the piston of the testing machine: the two arms of a strain gauge transducer (T) are equipped with fine needles (N and N′) which contact the calibrated part of the specimen on each edge of the calibrated part. The measurement of the shear γ is then free of errors due to the machine compliance. The net precision is about 0.005.

Simple shear was applied by the means of a special shearing stage actuated by the hydraulic ram of a MTS 810 universal testing machine. Testing was done at different temperatures (from -100 to $+150°$ C) and shear rates ($\dot{\gamma} = 3 \times 10^{-5}$ to 3×10^{-2} sec^{-1}).

2.4. Characterization techniques

Microscopic examination of the sheared specimens was made after the following unloading sequence: (i) interruption of the test at a given strain, (ii) release of the shear force over 30 min (to allow short term strain recovery); and (iii) measurements of the overall residual or "plastic" shear, γ_{pl}. The deformation process was first observed at large scale in specimens with different values of residual shear, γ_{pl}, by means of a macrophotographic Nikkon camera. In addition to this general inspection, the microscopic distribution of shear across the sample was studied by the technique indicated below. The flat polished face of "modified" samples was rubbed slightly on emery paper (grit

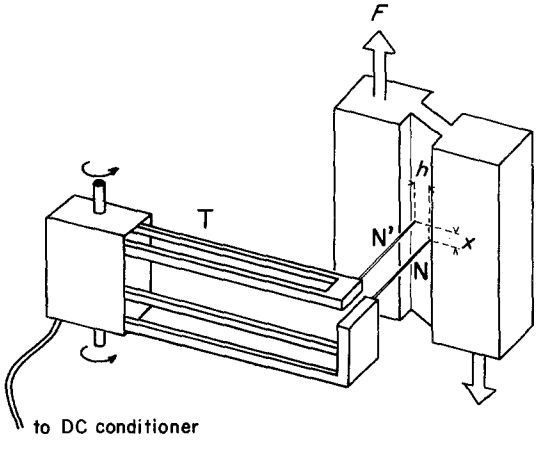

Figure 2 Shear transducer designed for the determination of the overall shear in the calibrated part of the specimens. (T, transducer; N and N′ needles in contact with the specimen.)

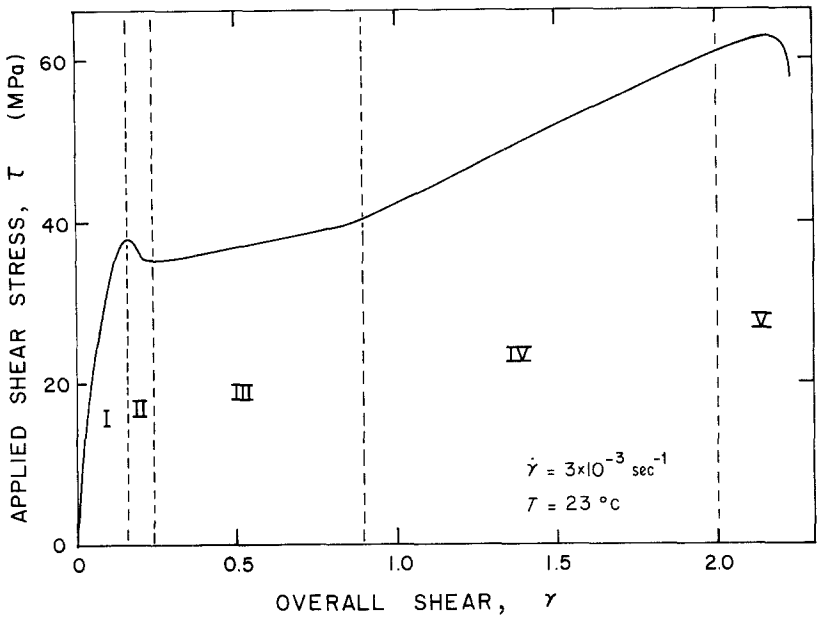

Figure 3 Typical experimental stress–strain curve obtained from a shear test on polycarbonate at room temperature (shear rate: $3 \times 10^{-3}\,\text{sec}^{-1}$).

1200 P) prior to the shear test so that an array of fine straight scratches was obtained perpendicular to the shear direction. The distortion of these markers was observed with a metallographic microscope (Reichert) after unloading at different steps of a shear test. The deviation angle, θ, of the scratches was measured in different locations over the surface of the calibrated part of the sample and served to quantify the *local* plastic shear ($\gamma_{Bpl} = \tan\theta$) with a resolution better than 3%. An inhomogeneous plastic deformation could be then characterized by a difference between the overall shear, γ_{pl}, and the local shear, γ_{Bpl}.

Macromolecular orientation was detected in deformed specimens by two methods: birefringence and X-ray diffraction. Sheared polycarbonate samples were observed between crossed polarizers in an optical microscope. Variation of the light transmission when the material is rotated denotes the anisotropy of refraction indices. The principal refraction axes coincide with the directions of extinction; they were determined as a function of the local plastic shear. X-ray diffraction patterns were also obtained with specimens strained to different values of residual plastic shear. A flat film camera was used, with a collimated filtered copper X-ray beam perpendicular to the $X0Y$ plane of the plate specimen. The diffracted intensity was measured directly from the film with a microphoto-densitometer. Its anisotropy also indicates the mean orientation of the macromolecules [18, 19].

3. Experimental results

3.1. Overall stress–strain behaviour of polycarbonate in simple shear

Fig. 3 shows an experimental stress–strain curve obtained from a shear test at room temperature (23° C) with a shear rate $\dot{\gamma} = 3 \times 10^{-3}\,\text{sec}^{-1}$. At this step, the mechanical behaviour of the shear specimens can be analysed, in a first approach, by taking into consideration (i) the fraction of short-term recoverability in the total deformation, and (ii) the apparent strain hardening measured from the current slope of the experimental stress–strain curve. On these grounds, the curve can be decomposed into five successive stages:

stage I is a region of viscoelastic response at strains smaller than about 0.15. The slope of the curve is about 420 MPa and decreases gradually due to anelastic response;

stage II corresponds to a stress drop beginning at an upper yield stress of 38 MPa. This stress drop has an amplitude of about 3 MPa. It extends over a shear strain increment of 0.1;

stage III is a region of plastic deformation

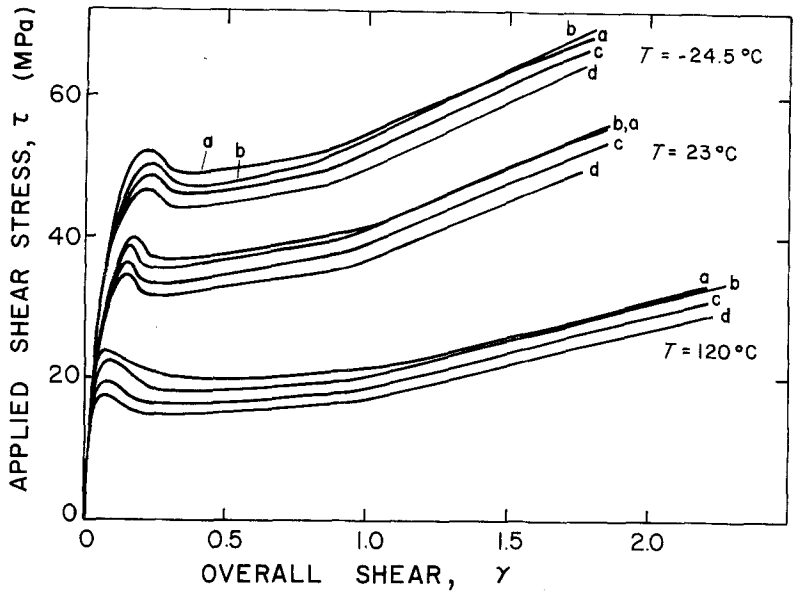

Figure 4 Influence of strain rate on the stress–strain behaviour of polycarbonate in simple shear. (a) $\dot{\gamma} = 3 \times 10^{-2}\,\text{sec}^{-1}$; (b) $\dot{\gamma} = 3 \times 10^{-3}\,\text{sec}^{-1}$; (c) $\dot{\gamma} = 3 \times 10^{-4}\,\text{sec}^{-1}$; (d) $3 \times 10^{-5}\,\text{sec}^{-1}$.

with a low value of strain hardening ($d\tau/d\gamma \simeq 7$ MPa), which is spread over a strain range from 0.3 to about 0.9. The value of the stress at which this stage ends (where there is a slope change in the curve) is approximately equal to the yield stress;

stage IV is a region of plastic deformation with a higher value of strain hardening ($d\tau/d\gamma \cong 18$ MPa). It extends over a strain range which varies a lot from one specimen to another, according to the occurrence of damaging phenomena. In the case of the specimen of Fig. 3, the stage ends at a strain of about 2.0 but other specimens ruined at a shear strain not larger than 1.6;

stage V is the rupture stage which starts by a gradual decrease of the slope of the τ–γ curve, becoming negative towards the end until a sudden stress drop signifies specimen rupture.

In the above decomposition, the definition of the stages is only phenomenological. We will examine in another section how they can be related to the microscopic evolution of the strain distribution in the specimen.

3.2. Effect of strain rate and temperature

The sensitivity of the plastic behaviour of polycarbonate to the shear rate is shown in Fig. 4, which displays the τ–γ curves obtained at four different strain rates from 3×10^{-5} to $3 \times 10^{-2}\,\text{sec}^{-2}$ at three temperatures (-24.5, $+23$ and $120°$ C). The increase of the plastic flow stress due to an increase of the strain rate is seen to be small, about 5% for one decade of strain rate. The overall strain rate sensitivity coefficient $m = (\partial \ln \tau/\partial \ln \dot{\gamma})_\gamma$ is thus of the order of 0.027. This value is similar to the strain rate sensitivity of polycarbonate in tension [3] and, generally speaking, of the same order to those of other glassy polymers such as polyvinyl chloride [17, 20].

The downward deviation at large strain of the curves obtained at the fastest shear rate (marked "a") is due to the adiabatic self heating which occurs in polymers at high strain rates. This phenomenon has already been observed in tensile tests (e.g. [21]) and during the simple shear testing of high density polyethylene [22].

The stress–strain curves given in Fig. 5 show that the plastic behaviour of polycarbonate is quite sensitive to temperature in the range -100 to $+150°$ C. It can be pointed out that the upper yield stress decreases gradually as temperature increases up to the glass transition temperature and then drops to zero. Stages II and III, which are well marked at low temperatures, becomes more and more diffuse at elevated temperature in such a way that the curve at 150° C is almost linear.

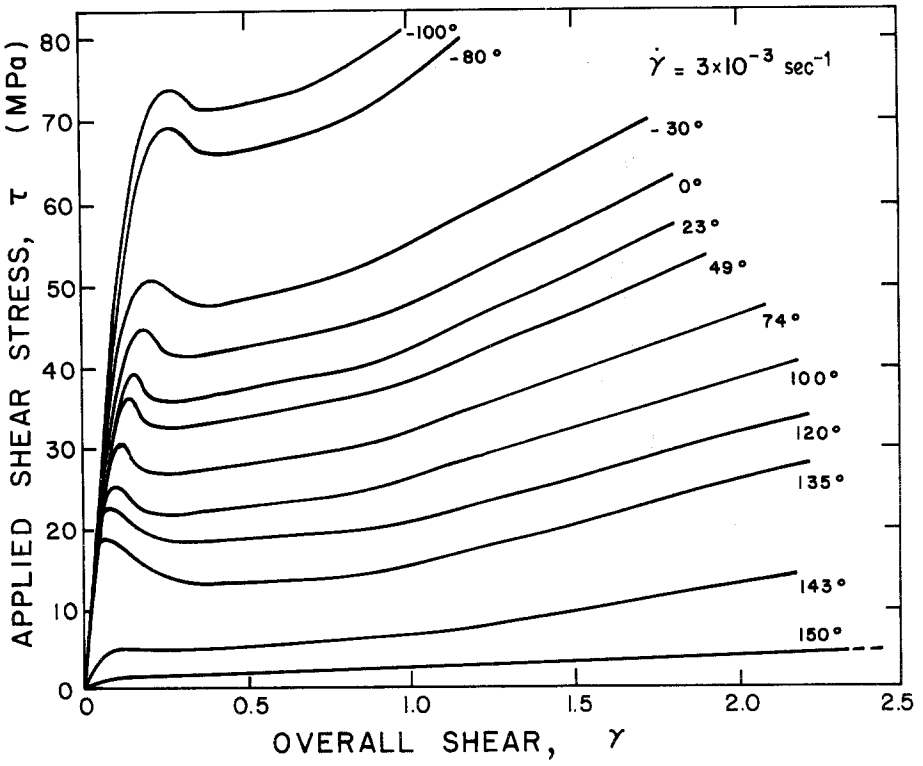

Figure 5 Influence of temperature on the stress–strain behaviour of polycarbonate in simple shear.

3.3. *In situ* observation of the deformation process

As we will demonstrate below, the different stages of the recorded stress–strain curve obtained at room temperature (Fig. 3) can be correlated to different steps in the development of shear banding within the specimen. This correlation was noted from observations at two different scales represented by the photographs in Figs. 6 and 7. Fig. 6 displays the overall aspect of several specimens deformed to increasing values of shear. Fig. 7 shows the enlarged photographs, at different deformation steps, of the central zone of one "modified" sample which had been marked with straight scratches prior to the test (Fig. 7a).

Stage I: homogeneous recoverable deformation. The whole calibrated part of the specimen deforms homogeneously in this stage. The strain is recovered within a short time as the stress is removed, and the overall shape, as well as the surface markings are then identical to those in the undeformed state, Figs. 6a and 7a.

Stage II: nucleation and elongation of one shear band. One shear band nucleates as the shear stress passes its maximum. It usually appears in the middle of the calibrated part of the test specimen; its width is of the order of 0.1 mm and its length is shorter than the specimen (Figs. 6b and 7b). The local residual shear, γ_{Bpl} within the band, as measured from the inclination of the marking scratches, is about 0.6. The termination of the shear at both ends of the band is not abrupt, as shown by the enlarged micrograph of Fig. 8: at the tip of the shear band the originally undeformed material shows a gradual transition giving way to the plastically deformed material. This transition spreads over a length of about 4 mm. During the complete duration of stage II, while the shear stress is gradually decreasing, the shear band grows in length until it becomes as long as the calibrated part of the specimen (Fig. 6c). By the same time, the width of the band increases slowly, such as the local shear within the band.

Stage III: widening of the shear band. After the band has reached the ends of the specimen (this occurs as the shear stress passes its minimum), its width increases equally to both sides until it occupies all the calibrated part of the sample. On the stress–strain curve, this

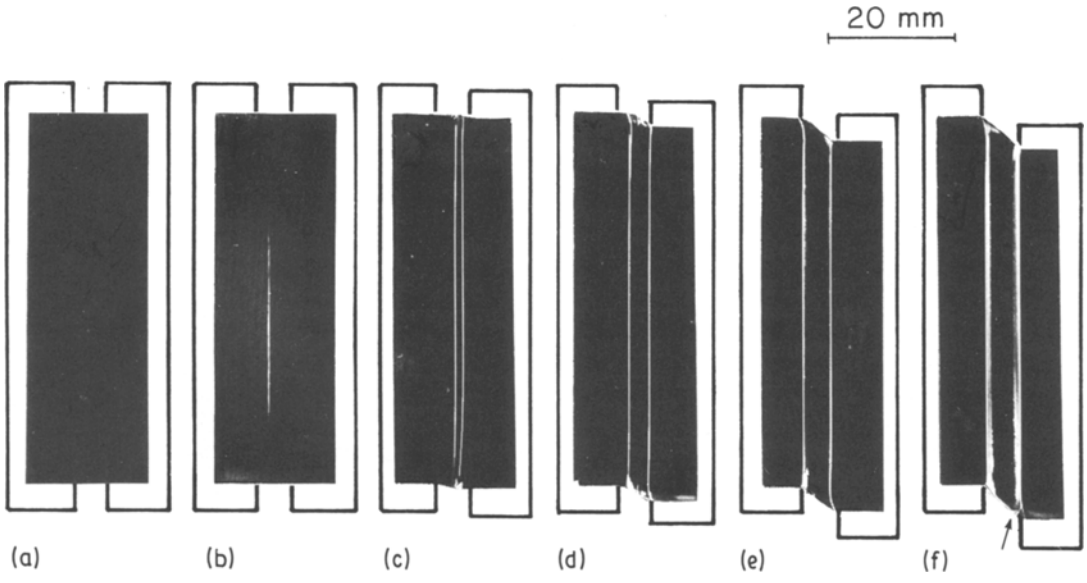

Figure 6 Overall macroscopic observation of polycarbonate specimens deformed to increasing values of shear (a) unsheared specimen; (b) just after load maximum, stage II; (c) and (d) stage III (e) stage IV; (f) initiation of a crack at the lower end of the specimen.

corresponds to the sort of plateau with a small strain hardening after the minimum of the stress. This stage is therefore a period of inhomogeneous deformation during which only the material in the shear band deforms plastically. The overall photograph of Fig. 6d, such as the detailed views of Figs. 7c and d, are characteristic of this state of evolution. It can be noted also that the plastic shear in the band goes on increasing slowly while the band is widening.

Stage IV: homogeneous plastic deformation. This stage corresponds to the portion of the stress–strain curve with a higher strain hardening. The band is now as wide as the calibrated portion of the specimen (4 mm). The overall shear is then equal to the local shear strain in the band, as in Figs. 7e and f. Until the end of stage IV, the major part of the specimen remains free of crazing. This is because simple shear develops a state of stress whose hydrostatic component is zero or very small, so that the crazing criterion is not fulfilled [15, 23]. However, while the deformation is increasing, some perturbations become visible in the peripheral regions: (i) the ends are curved in a convex way due to unbalanced internal stresses [15]; (ii) white zones develop along the edges, starting from the ends, which are made of a series of crazes perpendicular to the tensile principle axis of stress.

Stage V: rupture. After the progressive development of crazes, a crack is nucleated and propagates along the specimen. This takes place first at one end near the edge forming an outward corner (Fig. 6f). The rupture propagation process was identified by scanning electron microscope. Fig. 9a shows the tip of the growing crack. It is seen that before the separation proceeds, a series of small flaws are formed, presumably by extension of crazes. This crack propagated from the bottom to the top, incorporating the flaws which developed ahead of its tip. It was sometimes observed that the flaws had a diamond shape quite similar to those previously observed in glassy polymers fractured in tension [24]. After the separation was completed, the rupture face could be observed (Fig. 9b). It is characterized by a series of ridges and valleys all along the specimen edge. The enlarged view of the bottom of a valley makes evident the fibrillar nature of the fracture process, assessing the high toughness of polycarbonate at room temperature.

3.4. Uniformity of the strain within the band

The examination of surface markers on a deformed specimen (Fig. 7b to f) shows that their inclination within the band is very regular, denoting a uniform shear strain in this region. In order to check if the strain remains uniform in

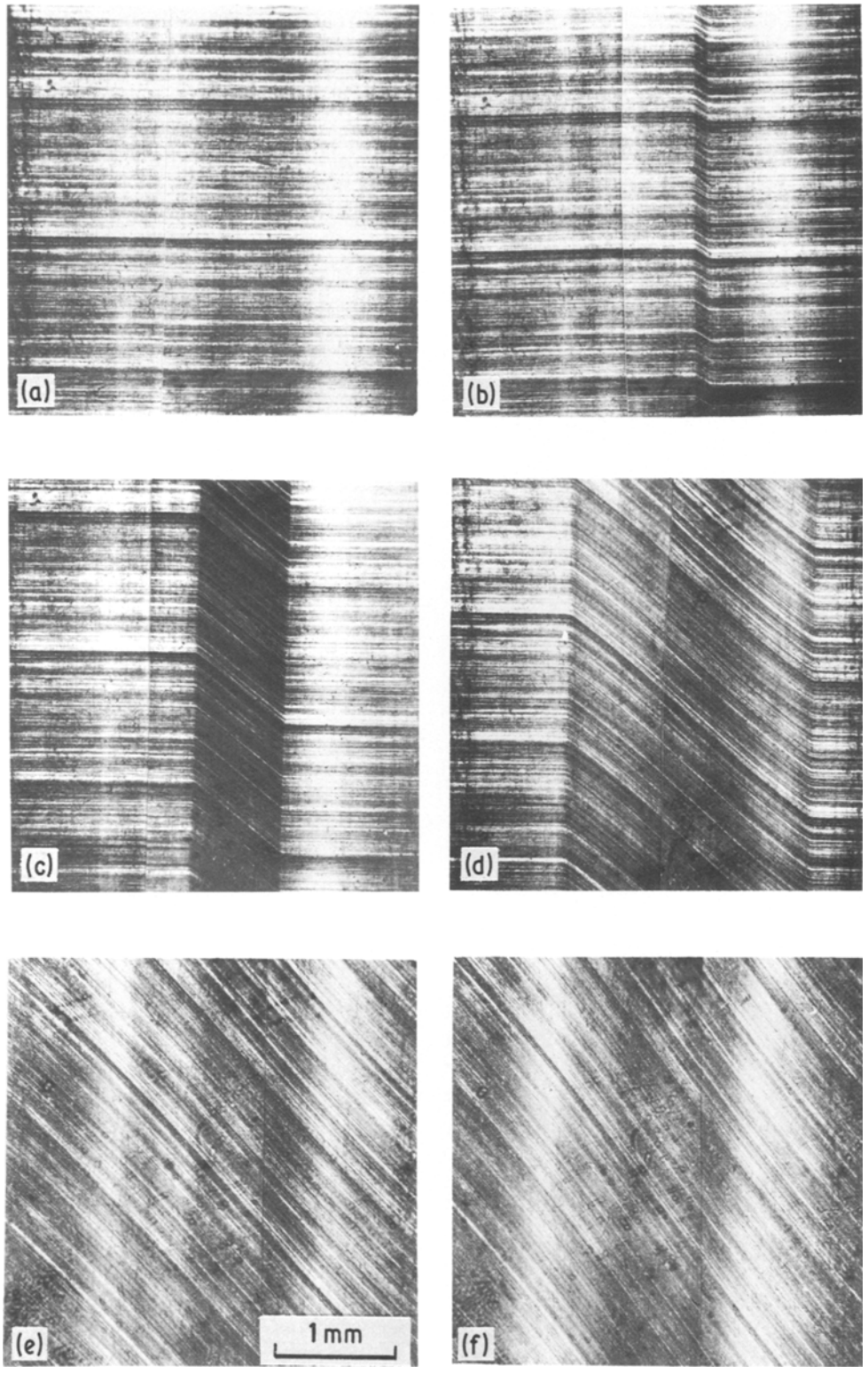

Figure 7 Microscopic observation of the development of a shear band in one polycarbonate specimen in simple shear. (a) Surface markers (scratches) on the unsheared sample; (b) stage II: the deviation of the markers assess the local shear; (c) and (d) widening of the band during stage III; (e) and (f) homogeneous shear during stage IV.

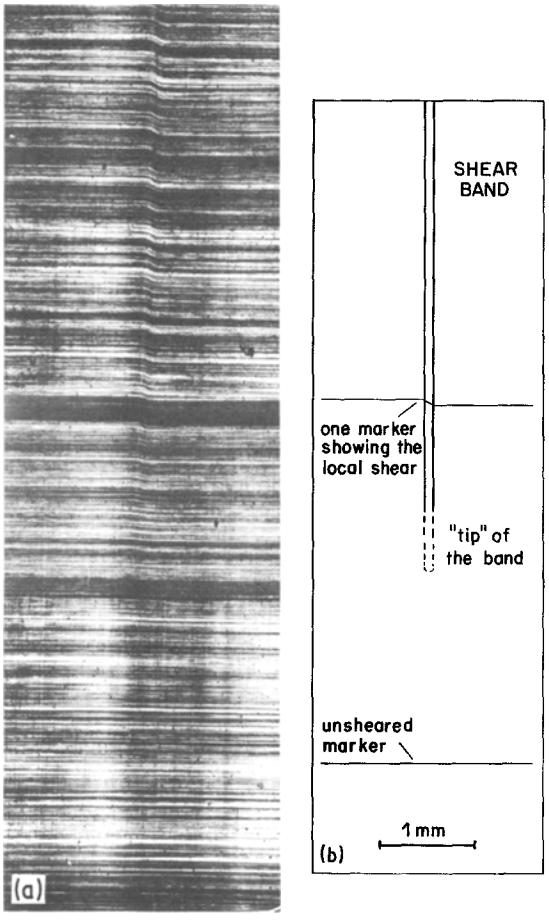

Figure 8 Detailed observation of the local distribution of plastic shear around the tip of an elongating shear band.

the band at a smaller scale, some specimens were polished to a specular aspect and then marked with extremely thin scratches by means of a tungsten needle which was moved perpendicular to the shear axis with a special chariot. The samples were then sheared at room temperature in the usual way. The scanning electron micrograph of Fig. 10a shows one of these markers on a shear band whose plastic deformation was $\gamma_{Bpl} = 0.71$. The marker is about 2 μm wide and it appears to be quite straight. Even at a higher magnification, Fig. 10b, the edge of the scratch still exhibits a nearly perfect rectitude. It can then be concluded from the matter above that the plastic deformation of polycarbonate is highly inhomogeneous during stages II and III at the scale of the overall specimen (one plastic shear band bordered by undeformed material) but that it is fairly uniform within the shear band, even at a scale as small as 100 nm.

3.5. Molecular orientation

Birefringence and X-ray diffraction techniques were applied to the plastically deformed material inside the band whose shear was determined from the markers method. All the measurements were made on specimens deformed in simple shear at room temperature and then unloaded for hours in order to take into account the molecular orientation due to the plastic deformation only.

The examination of a specimen in the polarized microscope showed that the shear band was highly birefringent ($\Delta n \cong 4 \times 10^{-2}$), due to the presence of polarizable benzene rings within the backbone of the chain. Consequently, the direction of maximum refractive index coincides with the mean direction of macromolecular orientation, unlike polystyrene whose benzene rings are pendant from the chains [25–28]. The angle of inclination between this principal direction and the shear axis $0X$ was determined for different values of the plastic strain. The results are plotted in Fig. 11 as triangles. The inclination angle decreases gradually with plastic shear (no measurement is available at small strains since the band gets a large shear as soon as it is formed).

While the wide-angle X-ray diffraction halo obtained on a flat film with an undeformed polycarbonate specimen is of isotropic intensity (Fig. 12a), the pattern obtained when the X-ray beam is collimated on to a shear band is characterized by an incomplete ring, as shown in Fig. 12b for $\gamma_{Bpl} = 1.4$. The direction of minimum intensity corresponds [18] to the mean orientation direction of the diffusing macromolecules. The angle between this direction and the shear axis was also plotted in Fig. 11 as open circles. It appears that results obtained from X-ray scattering are in good agreement with those deduced from birefringence measurements, confirming the gradual rotation of the mean orientation axis of the polymer chains toward the shear direction with plastic deformation.

4. Discussion

4.1. Kinetics of plastic instability

As we observed in the preceding section, a drop

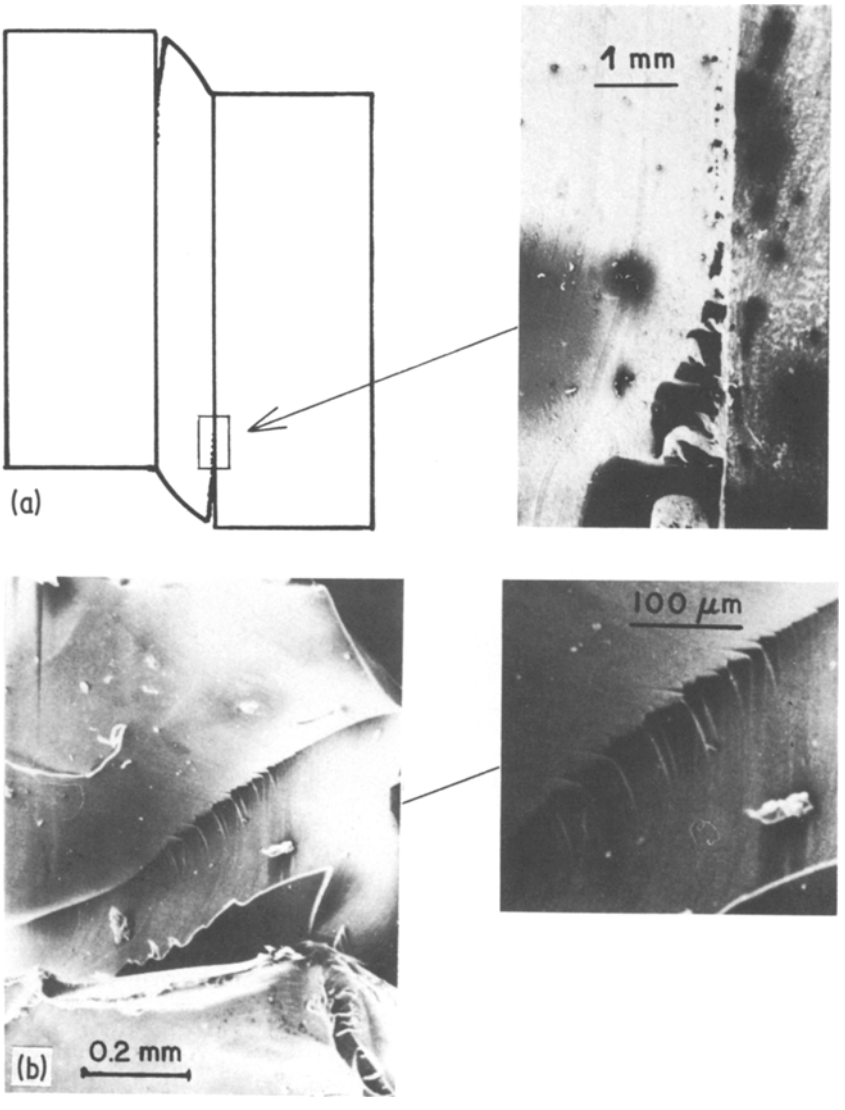

Figure 9 Scanning electron microscopic observation of the rupture faces of polycarbonate in simple shear. (a) Evidence of cavitation damage ahead of a crack growing from the lower specimen end. (b) Microfractographic observation of the rupture surface.

in the applied stress indicates the end of the viscoelastic stage during which the strain is distributed homogeneously over the whole calibrated portion of the specimen. It initiates, therefore, a period of inhomogeneous deformation. The shear stops growing all over the sample, except in the very limited volume of the appearing band which must accommodate alone the overall distortion imposed at a constant rate $\dot{\gamma}$ to the specimen. This abrupt mechanical bifurcation is a particular case of plastic instability which includes various phenomena such as diffuse necking of axi-symmetric specimens in tension, Lüders bands formation and localized necking in sheet materials subjected to plane strains [29]. However, the banding phenomenon observed in the present work is particularly simple since the geometry corresponds to the plain strain case. The local plastic shear along the band (γ_{Bpl}) can therefore be analysed from the observation of the local residual distortion of the surface markers. Also because the specimen does not exhibit any significant change of its cross section (*Le*), the observed yield drop during stage III cannot be the result of a geometrical softening, such as in diffuse or localized

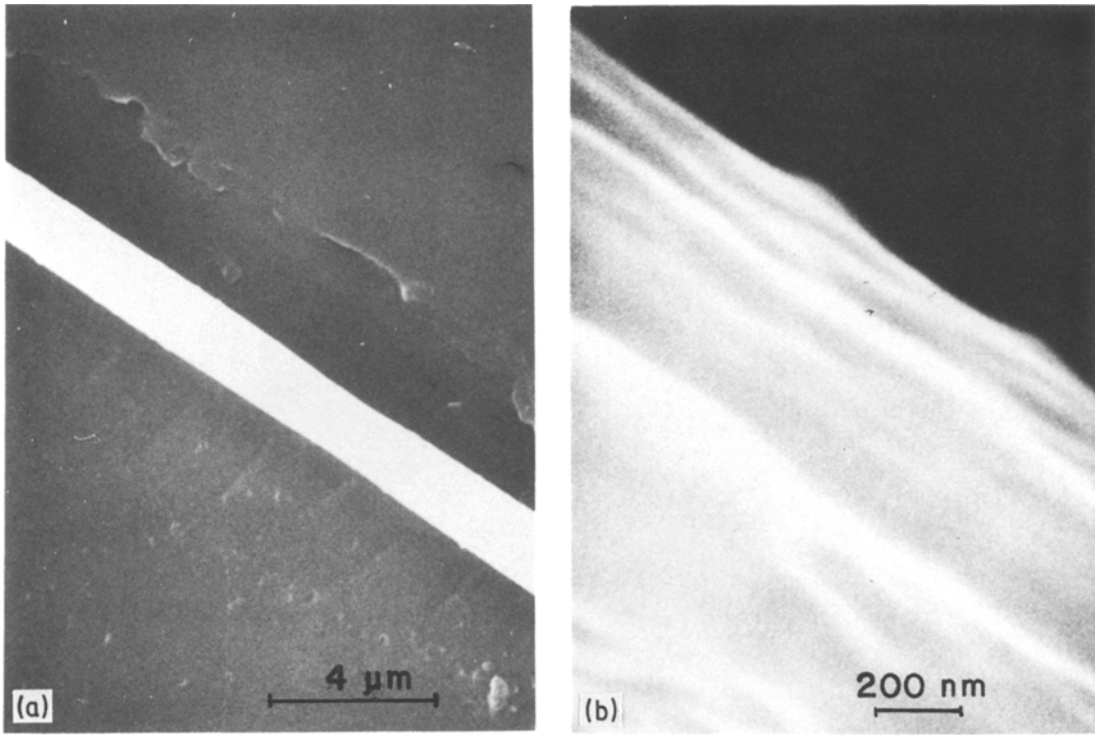

Figure 10 Scanning electron micrograph of a thin scratch marked on the surface of a shear band ($\gamma_{Bpl} = 0.71$).

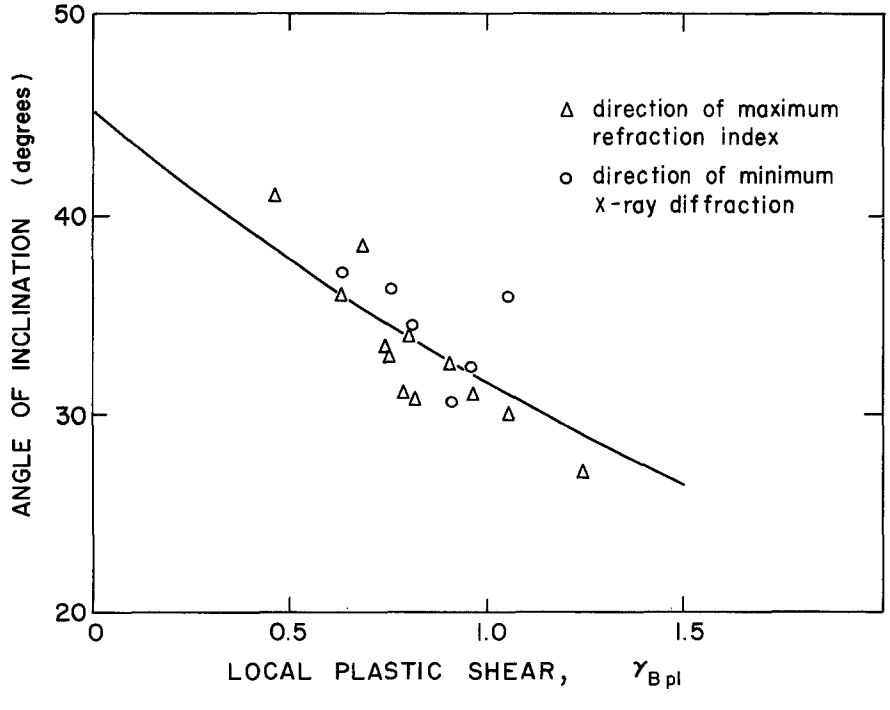

Figure 11 Inclination of the principal direction of macromolecular orientation as a function of local plastic shear in the band. Triangles refer to birefringence measurements, circles to X-ray diffraction. The solid line indicates the orientation of the principal direction of Eulerian strain tensor.

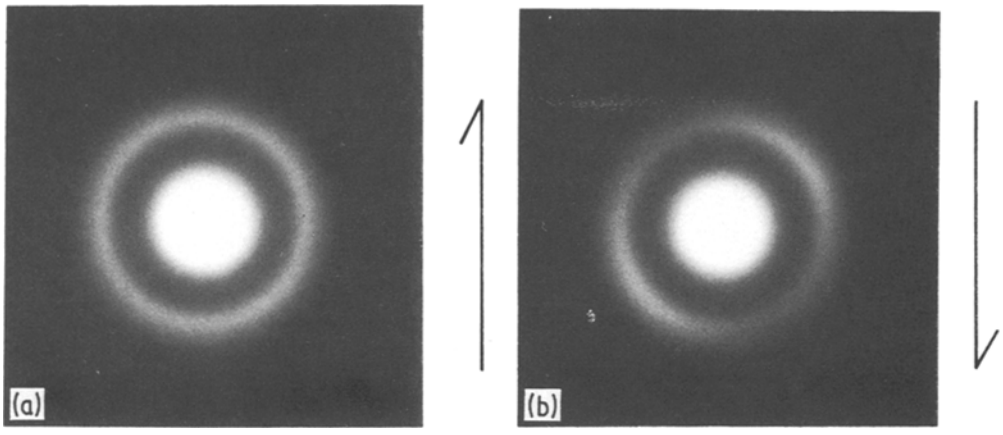

Figure 12 Flat film X-ray patterns obtained with (a) undeformed polycarbonate, and (b) polycarbonate sheared to a plastic strain $\gamma_{Bpl} = 1.4$.

necking; it is necessarily connected to a true softening of the sheared material [30] while the band is elongating toward the end. The ascending plateau in stage III corresponds to the steady transversal propagation of a straight deformation front which separates in an abrupt way the plastic shear band and the rest of the material which is still in its viscoelastic stage. This evolution is thus an experimental example of the shear instability problem studied theoretically by Bowden [31] and by Argon [32] in order to model on simpler bases the complex banding process observed in tension or compression in most glassy polymers. The mathematical treatment proposed by these authors describes the development of several shear bands of infinite length and predicts the gradual transfer of the applied shear into these sites of inhomogeneity. It is shown that shear banding is favoured if at least one of the following conditions is verified:

1. the specimen presents initially some unavoidable weaker zone acting as a band nucleation site similar to the cross-section defects for the diffuse necking of axisymmetrical tensile specimens [33];

2. the material exhibits an intrinsic strain softening after the yield point, that is its true stress–true strain curve in shear includes a stage of negative strain hardening (a thermal softening would produce a similar effect in the case of extensive adiabatic heating but it can be demonstrated [15] that the local variations of temperature are negligible at the slow strain rates used in this work);

3. the strain rate sensitivity $(\partial \ln \tau/\partial \ln \dot{\gamma})_\gamma$ is small enough to avoid that the excess of local strain rate when the band appears could impede the localization of shear;

4. the plastic strain hardening $(\partial\tau/\partial\gamma)_{\dot{\gamma}}$ is moderate.

In order to describe completely the kinetics of plastic instability in our simple shear test, we will first consider (Fig. 13) the general situation of a specimen containing under stress one localized shear band with a length L_B smaller than L and a width h_B smaller than h. The nominal (overall) strain can be decomposed, in a first approximation, into its elastic and plastic components

$$\gamma = \gamma_{el} + \gamma_{pl} \qquad (1)$$

The elastic strain is distributed all over the specimen and is roughly equal to $\gamma_{el} = \tau/M$

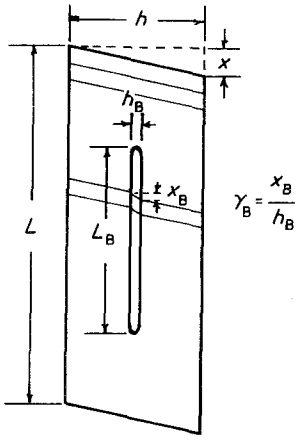

Figure 13 Definition of the various parameters concerned by the analysis of plastic instability in simple shear.

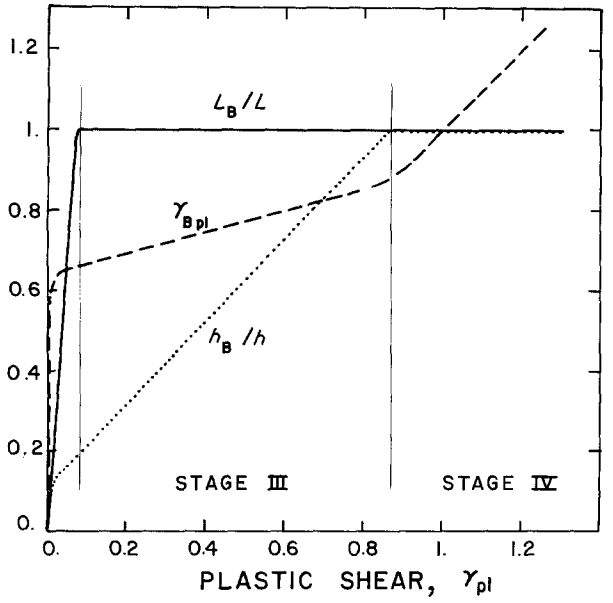

Figure 14 Evolution, during a simple shear test of polycarbonate, of the relative length of the band (L_B/L), of its relative width (h_B/h) and of the local plastic shear in the band (γ_{Bpl}).

where M is the apparent elastic modulus. Conversely, the plastic strain is concentrated in the band and can be written as proportional to the local displacement, x_B, in the band and its length L_B.

$$\gamma_{pl} = \frac{x_{Bpl}}{h}\frac{L_B}{L} = \frac{x_{Bpl}}{h_B}\frac{h_B}{h}\frac{L_B}{L}$$

$$= \gamma_{Bpl}\frac{h_B}{h}\frac{L_B}{L} \qquad (2)$$

As we impose the nominal strain rate $\dot{\gamma}$ in this test, one gets finally

$$\dot{\gamma} = \dot{\gamma}_{el} + \dot{\gamma}_{pl}$$

$$= \frac{\dot{\tau}}{M} + \gamma_{Bpl}\frac{h_B}{h}\frac{\dot{L}_B}{L} + \gamma_{Bpl}\frac{L_B}{L}\frac{\dot{h}_B}{h}$$

$$+ \frac{h_B}{h}\frac{L_B}{L}\dot{\gamma}_{Bpl} \qquad (3)$$

This expression includes the rate of evolution of the relative band length, L_B/L, of the relative band width, h_B/h, and of the plastic shear in the band, γ_{Bpl}. These parameters were determined experimentally from a number of tests and displayed in Fig. 14 as a function of γ_{pl}.

During stage I, no band is formed so that the only non-zero term in Equation 3 is the first term $\dot{\tau}/M$. In stage II the three curves in Fig. 14 exhibit an increase, but the one of L_B/L is far the steepest, so that the leading term in Equation 3 is the second term, $\gamma_{Bpl}(h_B/h)(\dot{L}_B/L)$. In the course of stage III, the length of the band is stabilized and both γ_B and (h_B/h) increase. However, the most significant term in the equation is the third one containing $\dot{h}_B/h$. Finally, when the band occupies all the calibrated part, the increase of γ is controlled entirely by the last term containing $\dot{\gamma}_{Bpl}$.

4.2. Relation between molecular orientation and shear strain

As we observed in the experimental section by birefringence measurements and X-ray diffraction (Fig. 11) the mean direction of molecular orientation rotates gradually with shear toward the shear axis $0X$ (Fig. 1).

On the other hand, it was demonstrated previously [15, 34, 35] that the principal axes of the strain ellipsoid in simple shear (principal directions of the Euler finite strain tensor) also rotate during a plane shear test. The angle α between the major (tensile) principal axis and the shear axis is given by the relation:

$$\alpha = \tfrac{1}{2}\tan^{-1}(2/\gamma) \qquad (4)$$

We have plotted the variation of α with γ in Fig. 11 by a full line curve. It can be seen that the value of α decreases with γ, starting from $\alpha = 45°$.

The comparison of the experimental data and the calculated curve in Fig. 11 shows that the agreement is fairly good within the limit of experimental errors. It can be stated, therefore,

that plastic deformation of glassy polycarbonate at room temperature forces the chains to orient along a mean direction parallel to the major principal axis of macroscopic local strain. This state of orientation subsists in the material after the stress is suppressed, as long as the specimen is not heated above the glass transition temperature. This "plastic" orientation of the macromolecules in a glassy polymer was previously discussed by several authors [36, 37] and compared to the recoverable chain orientation which is developed in rubbers subjected to hyperelastic deformation [38]. The orientation mechanism appears to be quite different for the two classes of materials. In the glassy state each elementary segment of macromolecule would orient itself as a small rigid stick embedded in a deforming continuum ("pseudo affine" model). Conversely, in the rubbery state, the overall deformation would be rather followed by the end-to-end vector of the freely jointed chains while the configuration of segments inside the chains would be determined by a criterion of maximum entropy ("affine" model). In the case of simple shear it was stated that both models support the observation that the principal axes of finite strains and the principal refraction axes rotate together [39]. However, on the bases of birefringence–strain curves reported in the literature [40] the rubber-like "affine" model is not likely to be applicable to glassy polycarbonate, since it would lead to much smaller values of birefringence than those which are measured, especially at moderate strains. Furthermore, the notion of freely jointed chains is highly inadequate to represent the macromolecules of polycarbonate at room temperature. It can then be thought that the "pseudo affine" model better describes the orientation process. Similar conclusions were drawn in the case of polystyrene in previous papers (e.g. [41]).

4.3. Derivation of a constitutive equation for the intrinsic plastic behaviour of polycarbonate

From the experimental data presented above, since both stages I and IV are characterized by the uniformity of shear, the experimental stress–strain curve in these stages can be taken for the description of the viscoelastic and steady-state plastic behaviour of the material, respectively. Conversely, the intermediate stages II and III correspond to non-uniform states of deformation for which the local shear strain and strain rate vary considerably with time and space; therefore, the corresponding portions of the recorded $\tau(\gamma)$ curve cannot be considered as representative of the material behaviour. The constitutive equation of polycarbonate between $\gamma = 0.2$ and $\gamma = 1.0$ should be obtained from the variation of the local shear stress in the band as a function of the local shear strain under constant local shear rate. Although this information is not available directly from the experiments, we saw above that the material within the band undergoes a gradual shearing at the tip of the band and then we can suppose in first approximation that the intrinsic (local) stress–strain curve can be extrapolated to the left from the linear portion of stage IV. At 23° C, for example, the curve for homogeneous deformation obtained from this extrapolation is represented as a dashed line in Fig. 15, for a constant shear rate $\dot{\gamma} = 3 \times 10^{-3}\,\mathrm{sec}^{-1}$. The extrapolated yield stress, τ^*, can be estimated to be about 25 MPa.

According to a number of previous studies on glassy polymer plasticity [3, 20, 42–45], the respective influence of strain, strain rate and temperature on the shear stress can be correctly represented by a constitutive equation of additive form:

$$\tau(\gamma, \dot{\gamma}, T) = \tau^*(\dot{\gamma}, T) - \tau_i(\gamma, T) \qquad (5)$$

In this model, the effect of a change of shear rate is to shift the stress–strain curve vertically, which is in good agreement with the result displayed in Fig. 4. The first term $\tau^*(\dot{\gamma}, T)$ of the equation (called the "effective" stress in the literature, e.g. [45–47]), controls the strain rate, through a relation of the following type $\dot{\gamma}(\tau^*, T) = \dot{\gamma}_0(T) \exp[V_a(T)\tau^*/kT]$. The apparent activation volume $V_a = kT(\partial \ln \dot{\gamma}/\partial\tau)_\gamma$ was determined from experimental curves such as those in Fig. 4. It is equal to about 4.7 nm^3 at room temperature, which corresponds to the total volume occupied by about fifteen bisphenol A carbonate nonomers. Measurements of strain-rate sensitivity at various temperatures between −30 and +120° C showed that $(\partial \ln \dot{\gamma}/\partial\tau)_\gamma$ is fairly constant in that range, so that the activation volume increases linearly with temperature (Fig. 16a). From the consideration above, the effective stress can be

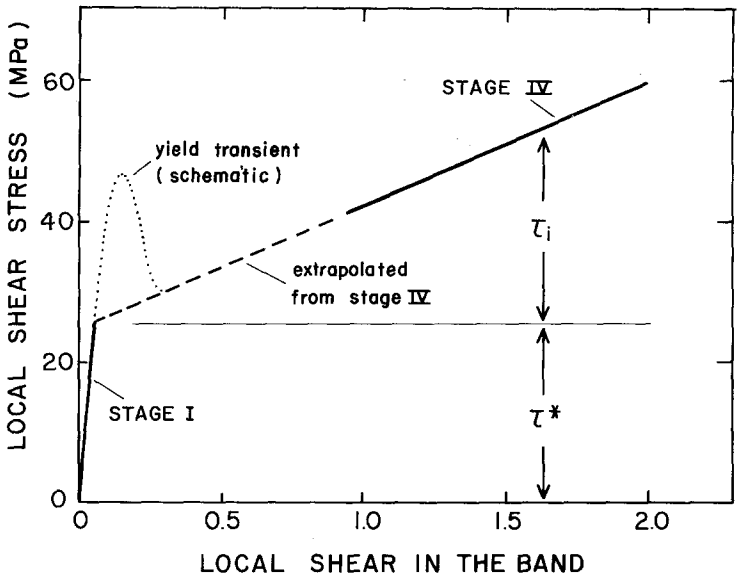

Figure 15 Intrinsic stress–strain curve of polycarbonate in simple shear at 23° C and $\dot{\gamma} = 3 \times 10^{-3}\,\mathrm{sec}^{-1}$. Portions in solid line correspond to the experimental data (stages I and IV of Fig. 3). The dashed line is extrapolated from the large strain steady state regime. The schematic peak at yield is tentatively presented to account for the initiation of plastic flow.

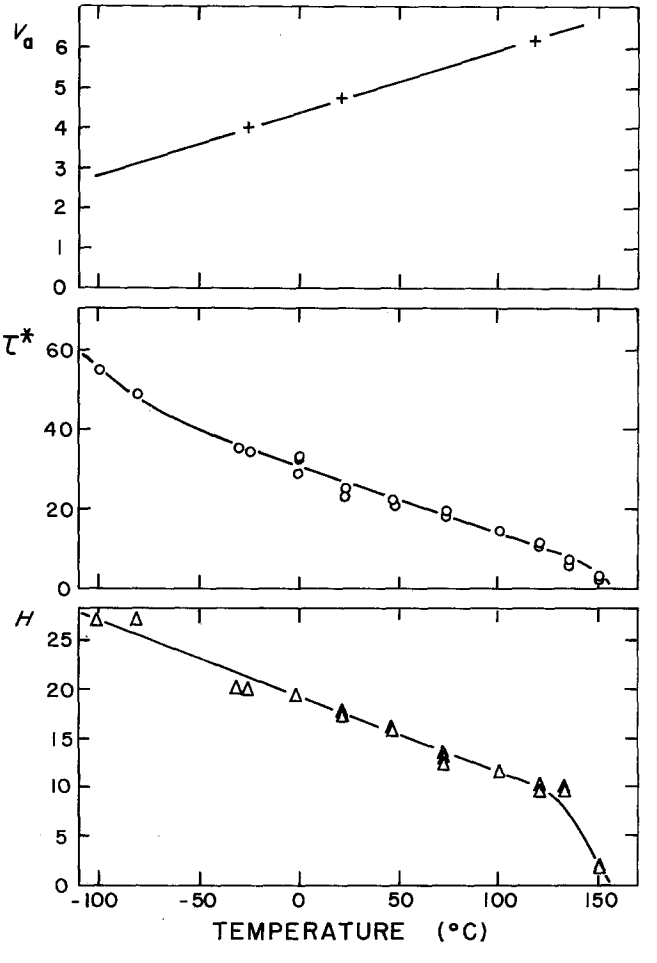

Figure 16 Dependence on temperature of the apparent activation volume, the "effective" stress and the strain hardening of polycarbonate in simple shear.

written following the equation

$$\tau^*(\dot{\gamma}, T) = \frac{kT}{V_a(T)} [\ln \dot{\gamma} - \ln \dot{\gamma}_0(T)] \quad (6)$$

Since the factor kT/V_a is constant, the overall influence of temperature τ^* (Fig. 16b) is due to the increase of the pre-exponential term $\dot{\gamma}_0(T)$ with temperature. The second term $\tau_i(\gamma, T)$ in Equation 5 is often referred to in the literature as the "internal" stress and measures the hardening caused by the accumulated plastic strain, as indicated in Fig. 15. It can be associated with the gradual orientation of the macromolecules in the deformed state. In contrast to the case of uniaxial tension [20] where the strain hardening of glassy polymers is exponential, the slope H of the τ_i–γ curve is constant in simple shear, so that the internal stress can be written simply

$$\tau_i(\gamma, T) = \gamma H(T) \quad (7)$$

The dependence of the hardening rate $H(T)$ on the absolute temperature is also displayed in Fig. 16c.

Although the above discussion provides us with a reliable description of the plastic behaviour of polycarbonate in steady state plastic flow, the constitutive equation of Equation 5 (as well as the linear τ–γ curve in Fig. 15) cannot be correct at the *initiation* of the plastic deformation. It has been proved indeed [13, 32, 48] that shear banding is likely to occur in a plastic material only if the intrinsic stress–strain curve presents a portion with negative slope (i.e. with strain softening). Since we noticed in the preceding chapter that the band appeared at yield in our specimens, it can be deduced that the curve in Fig. 15 should include a stress peak at small strains, as schematized qualitatively with a dotted line in agreement with previous studies on the transient plastic effects in glassy polymers subjected to uniaxial tension or compression [20, 47]. A detailed discussion on the origin and size of this peak will be the subject of another paper, based on the microstructural mechanisms which control the plasticity of polycarbonate in shear.

5. Conclusions

Plane simple shear tests were performed at different temperatures and different strain rates on amorphous polycarbonate. By quantitative *in situ* observation of the specimens, it was shown that a unique shear band is nucleated at the yield point which takes in all the plastic deformation. The band elongates and then widens steadily until all the specimen is brought up to a highly homogeneous shear equal to about unity. Lastly, the material deforms in a steady state uniform manner with a linear strain hardening and a gradual orientation of the macromolecules which align themselves along the major principal axis of finite strains, as assessed by optical and X-ray measurements. Rupture occurs by gradual crazing in the peripheral regions of the specimens. The kinetics of the enlarging shear band were discussed as a mechanism of plastic instability, taking into account the geometry of the band and the distribution of the local shear rate.

The intrinsic stress–strain relations can be derived by extrapolation from the steady state terminal stage. It is characterized by a large temperature dependence of the flow stress and by a small strain rate dependence (large activation volume). Lastly the transient plastic behaviour at yield was considered. Whereas it is proved that a true yield drop is necessary to explain the initiation of a band in simple shear, the precise determination of its shape and height will require further modelling.

References

1. C. J. BAUWENS-CROWET, J. C. BAUWENS and G. HOMES, *J. Polym. Sci.* **A2-7** (1969) 735.
2. *Idem, J. Mater. Sci.* **7** (1972) 176.
3. C. J. BAUWENS-CROWET, J. M. OTS and J. C. BAUWENS, *ibid.* **9** (1974) 1197.
4. G. TITOMANLIO and G. RIZZO, *Polymer* **21** (1980) 461.
5. P. B. BOWDEN and S. RAHA, *Phil. Mag.* **22** (1970) 463.
6. *Idem, ibid.* **29** (1974) 149.
7. C. C. CHAU and J. C. M. LI, *J. Mater. Sci.* **14** (1979) 1593.
8. *Idem, ibid.* **15** (1980) 1898.
9. *Idem, ibid.* **16** (1981) 1858.
10. *Idem, ibid.* **17** (1982) 652.
11. *Idem, ibid.* **17** (1982) 3445.
12. E. J. KRAMER, *J. Polym. Sci., Polym. Phys. Ed.* **13** (1975) 509.
13. W. WU and A. P. L. TURNER, *ibid.* **11** (1973) 2199.
14. S. C. SHRIVASTAVA, J. J. JONAS and G. CANOVA, *J. Mech. Phys. Sol.* **30** (1982) 75.
15. C. G'SELL, S. BONI and S. SHRIVASTAVA, *J. Mech. Phys. Sol.* **30** (1982) 75.
16. C. G'SELL, in "Plastic Deformation of Amorphous

and Semi-Crystalline Materials", edited by B. Escaig and C. G'Sell (Les Editions de Physique, Les Ulis, France, 1982) p. 13.
17. C. G'SELL and J. J. JONAS, *J. Mater. Sci.* **14** (1979) 583.
18. M. KAKUDO and N. KASAI, "X-ray Diffraction by Polymers" (Kodansha, Tokyo, 1972).
19. B. K. WAINSHTEIN, "Diffraction of X-rays by chain molecules" (Elsevier, Amsterdam, 1966) p. 356.
20. C. G'SELL and J. J. JONAS, *J. Mater. Sci.* **16** (1981) 1956.
21. I. H. HALL, *J. Appl. Polym. Sci.* **12** (1968) 731.
22. S. BONI, Thèse d'Ingénieur, CNAM, Nancy (1981).
23. S. S. STERNSTEIN and L. ONGCHIN, *Amer. Chem. Soc. Poly. Preprints* **10** (1969) 1117.
24. P. L. CORNES, K. SMITH and R. N. HOWARD, *J. Polym. Sci. Polym. Phys. Ed.* **15** (1977) 955.
25. N. J. MILLS, in "Polymer Science", edited by A. D. Jenkins (North Holland, Amsterdam, 1972) p. 490.
26. B. FALKAI and G. HINRICHSEN, *J. Polym. Sci. Polym. Symp.* **58** (1977) 225.
27. I. M. WARD, *Proc. Phys. Soc.* **80** (1962) 1176.
28. *Idem, J. Polym. Sci. Polym. Symp.* **58** (1977) 1.
29. C. G'SELL, in "Plastic Deformation of Amorphous and Semi-Crystalline Materials", edited by B. Escaig and C. G'Sell (Les Editions de Physique, Les Ulis, France, 1982) p. 375.
30. N. BROWN and I. M. WARD, *J. Polym. Sci.* **A-26** (1968) 607.
31. P. B. BOWDEN, *Phil. Mag.* **22** (1970) 455.
32. A. S. ARGON, in "The Inhomogeneity of Plastic Deformation" (American Society for Metals, Metals Park, Ohio, 1973) p. 161.
33. J. J. JONAS, N. CHRISTODOULOU and C. G'SELL, *Scripta Metall.* **12** (1978) 565.
34. G. R. CANOVA, S. SHRIVASTAVA, J. J. JONAS and C. G'SELL, in "Formability of Metallic Materials – 2000 A.D.", edited by J. R. Newby and B. A. Niemer (American Society for Testing and Materials, Metals Park, Ohio, 1982) p. 189.
35. J. C. JAEGER, "Elasticity, Fracture and Flow" (Chapman and Hall, London, 1969) p. 32.
36. O. KRATKY, *Kolloid Z.* **64** (1933) 213.
37. I. M. WARD, *Brit. J. Appl. Phys.* **18** (1967) 1165.
38. L. R. G. TRELOAR, *Trans. Faraday Soc.* **43** (1947) 277.
39. N. BROWN, R. A. DUCKETT and I. M. WARD, *J. Phys. D. Appl. Phys.* **1** (1968) 1369.
40. B. FALKAI and G. HINRICHSEN, *J. Polym. Sci. Polym. Symp.* **58** (1977) 225.
41. J. B. C. WU and J. C. M. LI, *J. Mater. Sci.* **11** (1976) 434.
42. E. PINK, *Mater. Sci. Eng.* **23** (1976) 275.
43. J. M. ANDREWS and I. M. WARD, *J. Mater. Sci.* **5** (1970) 41.
44. I. M. WARD, *ibid.* **6** (1971) 1397.
45. A. S. ARGON, *Phil. Mag.* **28** (1973) 839.
46. H. EYRING, *J. Chem. Phys.* **4** (1936) 283.
47. B. ESCAIG, in "Plastic Deformation of Amorphous and semicrystalline Materials", edited by B. Escaig and C. G'Sell (Les Editions de Physique, Les Ulis, Paris, 1982) p. 187.
48. S. L. SEMIATIN and J. J. JONAS, "Formability and Workability of Metals: Plastic Instability and Flow Localization" (American society for Metals, Metals Park, Ohio, 1984) p. 85.

Received 5 July
and accepted 15 October 1984